

Kinetic Instabilities in the Growth of One Dimensional Molecular Nanostructures

J. Ben Taylor and Peter H. Beton*

School of Physics and Astronomy, University of Nottingham, Nottingham, NG7 2RD, United Kingdom
(Received 3 July 2006; published 8 December 2006)

We develop a theory for the growth of one dimensional (1D) chains stabilized by anisotropic interactions, such as hydrogen bonding. Molecular chains are nucleated, grow, and may then undergo a kinetically driven transition to a two dimensional morphology. Kinetic Monte Carlo simulations show that extended 1D growth occurs between two temperature limits determined by two distinct kinetic instabilities. The limiting temperatures depend on interaction strength and deposition rate and, for a certain parameter range, 1D growth is completely suppressed.

DOI: [10.1103/PhysRevLett.97.236102](https://doi.org/10.1103/PhysRevLett.97.236102)

PACS numbers: 68.43.Jk, 81.15.Aa, 81.16.Dn

Anisotropic intermolecular potentials arising from hydrogen bonding, metal coordination, and dipolar coupling promote the formation of complex arrangements of molecules adsorbed on metallic and semiconductor surfaces [1–6]. Depending on the symmetry of the intermolecular potential it is possible to form rows [1,2], open networks [3–5], and clusters [6]. Kinetic effects play an important role in these processes which, under appropriate conditions, occur spontaneously and provide examples of surface-based molecular self-assembly. It is well known that kinetic effects control the dimensionality and morphology of growth of adsorbates which interact through isotropic bonding [7–10]. To date, the interplay between *anisotropic* molecular bonding and growth kinetics has not been explored, but a theoretical framework is now required for a fundamental understanding of the formation and temporal stability of self-assembled molecular nanostructures.

In this Letter we present a theoretical investigation of the growth morphologies which occur for uniaxially anisotropically bonded molecules and show that the resulting one dimensional (1D) nanostructures provide artificial edges at which further adsorbed molecules may be temporarily bound. A combination of fast edge diffusion [10–12] and the corner (1D Schwoebel) barrier [13–16] encountered at the end of the molecular rows, leads to a competition between 1D growth and nucleation events which trigger a transition to two dimensional growth. We find that extended 1D molecular rows, stabilized by anisotropic interactions, are kinetically stable only over a finite temperature range.

Kinetic effects are modeled using established Monte Carlo schemes [17–19], modified through the introduction of a uniaxially anisotropic intermolecular potential [Fig. 1(a)]. Adsorbate diffusion is simulated by allowing molecules to hop from site to site on a hexagonal grid. Diffusion trajectories are calculated [20] as the minimum energy pathway (MEP) across the potential energy surface due to the isotropic van der Waals interactions arising from occupied nearest neighbor sites (defined as

the eight sites adjacent to the initial and final positions for a particular transition). We assume a Lennard-Jones pair potential with an equilibrium separation equal to the lattice constant of the hexagonal net and binding energy E_{VDW} . To take account of the anisotropic potential, the diffusion barrier height derived from the MEP is increased by E_{HB} ($2E_{HB}$), if the molecule is diffusing from a site which is stabilized by one (two) hydrogen bonds through alignment of nearest neighbor molecular axes. It is assumed that molecule-substrate interactions are weak and do not contribute to the diffusion barrier. This approach is significantly different from previous computational studies of directional growth for which a strongly anisotropic substrate is assumed [21–23].

The simulation of long time scales was implemented following Refs. [17,18,24]. The probability for molecule i to hop to site r is taken to be proportional to the Arrhenius hopping rate, $\nu_i^r = \nu_0 \exp(-E_i^r/kT)$, where E_i^r is the diffusion barrier and ν_0 is the barrier attempt frequency. The

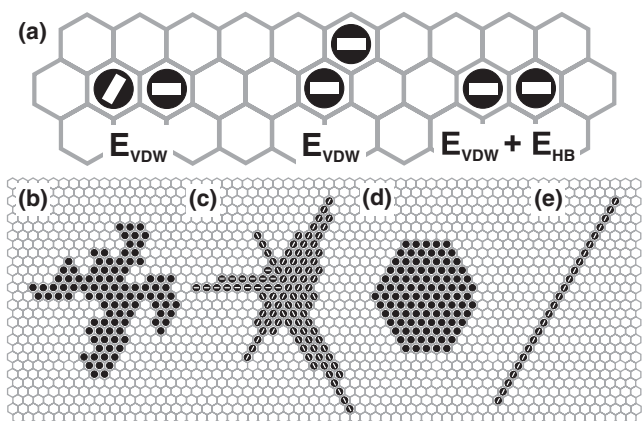


FIG. 1. (a) E_{VDW} and E_{HB} —isotropic and anisotropic binding energies (alignment illustrated by bars). (b)–(e) Variation of cluster morphology with anisotropic forces: $R = 10^{-15} \nu_0 \text{ MLs}^{-1}$, $T = 100 \text{ K}$; (b) $E_{VDW} = 520 \text{ meV}$, $E_{HB} = 0$; (c) $E_{VDW} = E_{HB} = 260 \text{ meV}$; (d) $E_{VDW} = 130 \text{ meV}$, $E_{HB} = 0$; (e) $E_{VDW} = 130 \text{ meV}$, $E_{HB} = 260 \text{ meV}$.

mean hopping rate for a simulated molecule is then the sum of the rates for transitions to all unoccupied neighboring sites. The overall occurrence of events in the system, ν_{tot} , is the average rate of deposition plus the sum of the hopping rates for all molecules, $\nu_{\text{tot}} = RA + \sum_{i,r} \nu_i^r$, where R is the deposition rate in monolayers (ML) per second and A is the number of simulated lattice points. The simulated system evolves sequentially through the random selection of events, chosen according to the event frequency weighted by ν_{tot}^{-1} . After each event, the simulated ensemble is updated through movement of the selected molecule i to site r , or the deposition of a new molecule onto an unoccupied site chosen at random. All results were calculated using a lattice of 100×100 points with periodic boundary conditions.

Adsorbate rotations are handled separately, after each diffusion event. A molecular axis is free to rotate until an anisotropic bond is formed, upon which the axis is rendered immobile. Once this and any other anisotropic bond has been broken (through translational motion), it is again unfixed in orientation. If any such axis can rotate to form an anisotropic bond, it is considered to do so spontaneously, with any choices in bonds or molecule rotations made randomly.

We first consider qualitatively the influence of anisotropic interactions upon cluster morphology. Figure 1(b) shows a simulated cluster formed by molecules with isotropic interactions. The introduction of an anisotropic interaction [Fig. 1(c)] results in the preferential growth and alignment of molecular axes along the principal directions of the lattice. Figures 1(d) and 1(e) demonstrate the effect of introducing anisotropic forces with weaker isotropic forces. In Fig. 1(e) cluster growth is biased to the point that purely 1D rows are formed.

The occurrence of 1D structures, such as Fig. 1(e), are of particular interest. To this end, simulations were performed to monitor the point at which a transition from purely 1D to 2D growth occurred. Results from these simulations are given in Fig. 2, which shows the probability of forming a purely 1D structure as a function of the number of deposited molecules, over a range of temperatures. For these calculations, $E_{\text{VDW}} = 200$ meV, $E_{\text{HB}} = 600$ meV, and the deposition rate was set as $R = 10^{-15} \nu_0 \text{ MLs}^{-1}$, corresponding to 0.01 MLs^{-1} for $\nu_0 = 10$ THz. The probabilities for each temperature were obtained by averaging over 1000 simulations. We find pure 1D growth only in a limited range of temperatures with upper and lower bounds T_H and T_L . As we show below, 1D growth is kinetically unstable outside this temperature range.

Figure 2(a) shows results for high temperatures, $T > T_H$. The upper curve shows that for $T = 290$ K pure 1D growth is obtained. As the temperature is increased the probability of 1D growth falls rapidly due, primarily, to the mechanism identified in the inset to Fig. 2(a). In this process, referred to as Type I, nucleation occurs between two molecules

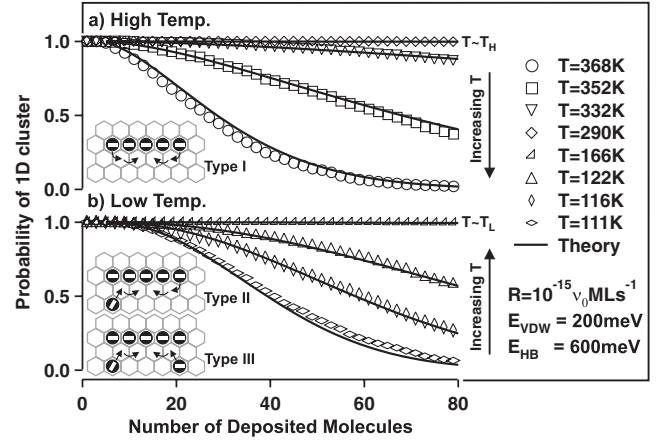


FIG. 2. Probability of forming a 1D cluster (see inset for parameters) for different growth temperatures. Symbols correspond to simulations and continuous curves to theory (see text). In the range 166 K–290 K the growth is 1D. Insets show three mechanisms which limit pure 1D growth through the nucleation of new rows.

which hop off the end of the 1D cluster, over an energy barrier equal to E_{HB} , and diffuse along the edge of the line. If two such molecules meet, the nucleation of a new line occurs. This line grows along the edge of the preexisting 1D cluster and the growth is no longer classified as purely 1D. This process is independent of deposition rate and, in the absence of deposition, controls the temporal stability of 1D lines.

Figure 2(b) shows results for a low temperature regime, $T < T_L$. Again, the uppermost curve, $T = 166$ K, shows that pure 1D growth occurs. However, in this case the probability of 1D clusters falls as the temperature is *reduced*, rather than increased as in Fig. 2(a). The transition away from pure 1D growth occurs through the mechanism, denoted Type III [see Fig. 2(b) inset]. Here the relevant nucleation event is driven by two molecules which have been captured on the edge of the preexisting 1D cluster and are diffusing along its length, but have not yet been absorbed onto the cluster end. Unlike the Type I mechanism this process is strongly dependent on deposition rate. A further mechanism termed Type II, which is a hybrid of the Type I and Type III processes, can also occur but is only significant within the parameter range where T_L and T_H converge to a common value (see below).

These mechanisms are distinguished by three important time scales: (i) τ_{dep} the average time between deposition events, (ii) τ_{on} the average time a molecule spends on the side of a line before hopping onto the row end, (iii) τ_{off} the average time before a molecule hops off an end onto the cluster edge. The latter two time scales, and associated energy barriers, are illustrated in Fig. 3(a).

At high temperatures ($T > T_H$) Type I thickening is prevalent. As the temperature is decreased ($T_L < T < T_H$), the hopping of molecules off the end of the line slows

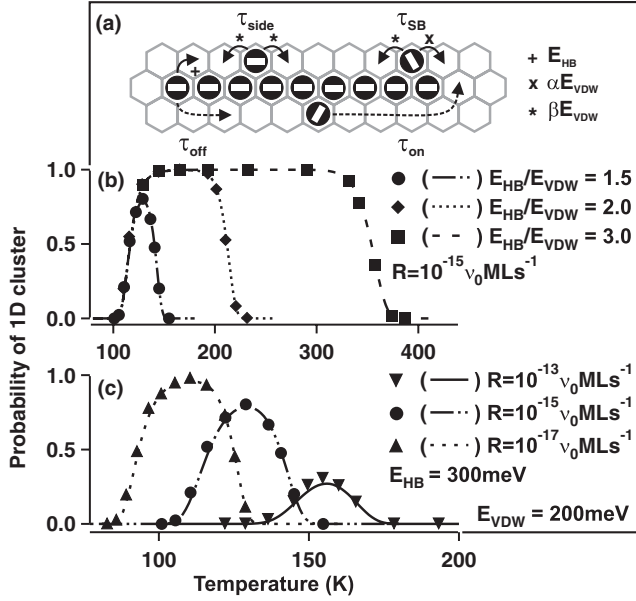


FIG. 3. (a) Schematic showing characteristic times (τ_{SB} , τ_{side}) and associated barriers (+, X, *) for single translation steps along edge of 1D line (α and β are constants discussed in text). Time scales τ_{on} and τ_{off} also identified schematically. (b) and (c) show the temperature dependence of forming 1D clusters composed of 60 molecules with varying (b) anisotropic bond strength and (c) deposition rate for fixed $E_{\text{HB}} = 300 \text{ meV}$. Symbols show the results of simulations, with the lines giving the associated theoretical curves [Eq. (8)].

exponentially ($\tau_{\text{off}} \rightarrow \infty$) and the Type I process is suppressed. In this regime deposited molecules become bound to and diffuse along the edge of the row and may still hop over the 1D Schwoebel barrier to the row end. Through this process the line continues to grow. However, at low temperatures ($T < T_L$) additional molecules are, on average, adsorbed on the row edge before diffusion onto the row end can occur, resulting in a Type III process. This is due to the long characteristic time for diffusion along the cluster edge and the high probability of reflection by the 1D Schwoebel barrier at the row end ($\tau_{\text{on}} \rightarrow \infty$).

In Fig. 2 we also plot theoretical predictions for the probability of 1D growth, based on a calculation of the probabilities, p_I , p_{II} , and p_{III} for the nucleation events governed by the Type I, Type II, and Type III mechanisms, respectively. The excellent agreement between the theory and simulations confirms that the mechanisms we identify control the kinetic stability of 1D growth.

Our theoretical curves are derived under the two primary assumptions that the time for a free molecule to be captured by a cluster is negligible and that molecules do not hop away from a cluster once captured by a side or end. Within these assumptions τ_{off} and τ_{on} are given by Eqs. (1) and (2), respectively.

$$\tau_{\text{off}} = [2\nu_0 \exp(-E_{\text{HB}}/kT)]^{-1} \quad (1)$$

$$\tau_{\text{on}} = n\tau_{\text{side}} + n(\tau_{\text{SB}} - \tau_{\text{side}})/(N - 2). \quad (2)$$

With respect to Eq. (1) the factor of 2 accounts for the four possible transitions (two from each end) and a geometric factor which results from the fact that, for the choice of a hexagonal array, a molecule crossing the barrier E_{HB} is temporarily stabilized in an intermediate site before either hopping back onto the end or, with equal probability, onto the cluster edge (see Fig. 3). The time scale τ_{on} , comparable to the form proposed in Ref. [16], is a function of the number of molecules forming the 1D line, N . τ_{side} and τ_{SB} are the average residence times for a molecule hopping between equivalent sites on the row edge and a molecule hopping away from a site at the end of a row edge, respectively [see Fig. 3(a)]. Explicitly,

$$\tau_{\text{SB}} = \nu_0^{-1} \left[\exp\left(-\frac{\alpha E_{\text{VDW}}}{kT}\right) + \exp\left(-\frac{\beta E_{\text{VDW}}}{kT}\right) \right]^{-1} \quad (3)$$

$$\tau_{\text{side}} = \nu_0^{-1} \left[2 \exp\left(-\frac{\beta E_{\text{VDW}}}{kT}\right) \right]^{-1}. \quad (4)$$

The coefficients α and β are geometric factors determined by the shape of the isotropic potential and for the Lennard-Jones form considered here are $\alpha = 0.927$, $\beta = 0.593$ (note that $\alpha > \beta$). The parameter n in Eq. (2) is the average number of molecular steps before capture by the end of the line and can be calculated using finite difference equations [25,26], yielding $n = 2(N - 2)(1 - \gamma)/\gamma + 1$, where $\gamma = \nu_0 \tau_{\text{SB}} \exp(-\alpha E_{\text{VDW}}/kT)$ is the probability of crossing the Schwoebel barrier.

Assuming events can be modeled by Poisson statistics, p_X , representing the probability of a 1D line undergoing a Type X transition before the addition of another molecule, may be written as

$$p_I \approx 1 - \exp\left(-\frac{p_c \tau_{\text{dep}}}{\tau_{\text{on}} + \tau_{\text{off}}}\right) \quad (5)$$

$$p_{II} \approx 0.5 p_{\text{meet}} p_{\text{edge}} \left[\frac{\tau_{\text{on}}}{\tau_{\text{on}} + \tau_{\text{off}}} + 1 - \exp\left(-\frac{\tau_{\text{on}}}{\tau_{\text{off}}}\right) \right] \quad (6)$$

$$p_{III} \approx 0.5 p_{\text{meet}} p_{\text{edge}}^2 \int_0^\infty \frac{1}{\tau_{\text{dep}}} \exp\left(-\frac{t}{\tau_{\text{dep}}}\right) \exp\left(-\frac{t}{\tau_{\text{on}}}\right) dt. \quad (7)$$

Here we have introduced the probabilities $p_{\text{meet}}(N) \approx (1 + \sum_{a=2}^{N-2} [1 + (a-1)/(2\gamma^{-1} - 2)]^{-1})/(N-2)$ [25,27], $p_{\text{edge}}(N) = (2N+1)/(2N+7)$ (~ 1 for large N), and $p_c(N) = 0.5 p_{\text{meet}}(N-1)[1 - \exp(-\tau_{\text{on}}(N)/\tau_{\text{off}})]$. These represent, respectively, the probability that two molecules on the side of a cluster will meet, the probability that a deposited molecule will be captured by an edge (as opposed to an end) of a 1D cluster, and the conditional probability that a Type I process will occur if a molecule is already adsorbed on the row edge.

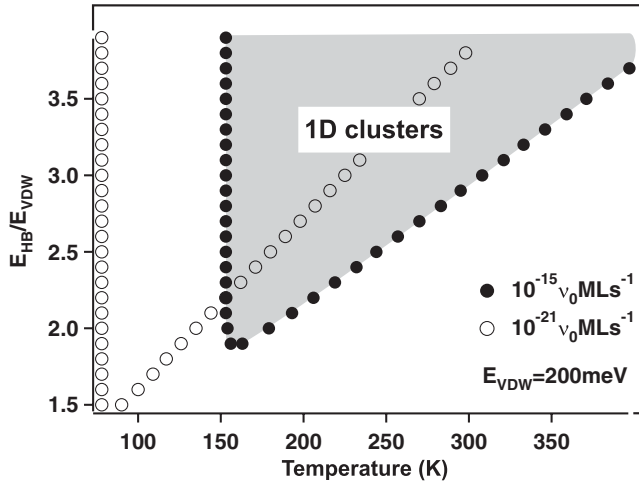


FIG. 4. Regions of stable 1D growth.

Defining the probability of a line of length N thickening by any mechanism before a deposition event results in the lengthening of the line, $P(N) = p_I + p_{II} + p_{III}$, the probability of obtaining a 1D cluster of length N , $P^{1D}(N)$, is

$$P^{1D}(N) = 1 - \sum_{N'=2}^N \left[P(N') \prod_{i=1}^{N'-1} 1 - P(i) \right]. \quad (8)$$

This expression, which contains no free parameters, is plotted in Fig. 2.

Further simulations have been undertaken to determine the dependence of T_L and T_H on deposition rate and anisotropic bond strength. Strictly, these bounding temperatures are dependent on the length of the 1D line, but for long lines the dependence is weak. The probability of obtaining a 1D cluster for $N = 60$ is plotted against temperature for varying anisotropic bond strengths [Fig. 3(b)] and deposition rates [Fig. 3(c)]. The temperature T_L is unaffected by varying E_{HB} , since Type III thickening is independent of anisotropic bonding. Conversely, T_H decreases as E_{HB} decreases. In fact, the temperature range over which 1D clusters are formed vanishes for E_{HB}/E_{VDW} below ~ 1.8 . In this case, the Type I to Type III transition is bridged by Type II thickening. The region of stable 1D growth ($T_L < T < T_H$) is also dependent on the deposition rate [Fig. 3(c)]. A lower deposition rate gives rise to a reduction in both T_L and T_H , since the time available for edge diffusion increases, reducing the probability of Type III thickening but increasing the chances of Type I thickening.

Figure 4 more clearly demonstrates the conditions for which 1D growth (as described for Fig. 3) is expected, for varying temperatures and anisotropic interactions. These conditions are represented by the shaded region for which $R = 10^{-15} \nu_0 \text{ MLs}^{-1}$. Also shown are the boundaries for the equivalent region for $R = 10^{-21} \nu_0 \text{ MLs}^{-1}$.

Overall our results confirm that growth of 1D nanostructures is induced by uniaxially anisotropic intermolecular interactions. However, while anisotropic forces are important, they do not necessarily lead to 1D structures. A crucial role in the 1D growth process is also played by temperature and deposition rate. While our discussion has been focussed on a particular class of surface-based self-assembly, we note that many molecular adsorbates have strongly anisotropic interactions. Our approach is therefore likely to have wider relevance to the morphology and dimensionality of organic thin film growth.

We thank the UK Engineering and Physical Sciences Research Council for financial support through Grant No. GR/S97521/01. We also thank George Johnson for useful discussions in the early stages of this work.

*Electronic address: ppzphb@nottingham.ac.uk

- [1] J. V. Barth *et al.*, *Angew. Chem., Int. Ed.* **39**, 1230 (2000).
- [2] D. L. Keeling *et al.*, *Nano Lett.* **3**, 9 (2003).
- [3] J. A. Theobald *et al.*, *Nature (London)* **424**, 1029 (2003).
- [4] S. Griessl *et al.*, *Single Mol.* **3**, 25 (2002).
- [5] S. Stepanow *et al.*, *Nat. Mater.* **3**, 229 (2004).
- [6] T. Yokoyama *et al.*, *Nature (London)* **413**, 619 (2001).
- [7] H. Brune, *Surf. Sci. Rep.* **31**, 121 (1998).
- [8] J. G. Amar, F. Family, and P.-M. Lam, *Phys. Rev. B* **50**, 8781 (1994).
- [9] G. S. Bales and D. C. Chrzan, *Phys. Rev. Lett.* **74**, 4879 (1995).
- [10] Z. Zhang and M. G. Lagally, *Science* **276**, 377 (1997).
- [11] M. V. R. Murty and B. H. Cooper, *Phys. Rev. Lett.* **83**, 352 (1999).
- [12] C. Ratsch, M. C. Wheeler, and M. F. Gyure, *Phys. Rev. B* **62**, 12 636 (2000).
- [13] G. Ehrlich and F. G. Hudda, *J. Chem. Phys.* **44**, 1039 (1966).
- [14] R. L. Schwoebel, *J. Appl. Phys.* **40**, 614 (1969).
- [15] O. Pierre-Louis, M. R. D'Orsogna, and T. L. Einstein, *Phys. Rev. Lett.* **82**, 3661 (1999).
- [16] J. Zhong *et al.*, *Phys. Rev. B* **63**, 113403 (2001).
- [17] A. F. Voter, *Phys. Rev. B* **34**, 6819 (1986).
- [18] A. C. Levi and M. Kotrla, *J. Phys. Condens. Matter* **9**, 299 (1997).
- [19] M. Kaukonen *et al.*, *Phys. Rev. B* **61**, 980 (2000).
- [20] G. Henkelman, B. P. Uberuaga, and H. Jónsson, *J. Chem. Phys.* **113**, 9901 (2000).
- [21] M. A. Albao *et al.*, *Phys. Rev. B* **72**, 035426 (2005).
- [22] C. Mottet *et al.*, *Surf. Sci.* **417**, 220 (1998).
- [23] Y. M. Mo *et al.*, *Surf. Sci.* **219**, L551 (1989).
- [24] A. B. Bortz, M. H. Kalos, and J. L. Lebowitz, *J. Comput. Phys.* **17**, 10 (1975).
- [25] W. Feller, *An Introduction to Probability Theory and its Applications* (Wiley, New York, 1968), 3rd ed.
- [26] M. A. El-Shehawey, *J. Phys. A* **33**, 9005 (2000).
- [27] C. A. Walsh and J. J. Kozak, *Phys. Rev. Lett.* **47**, 1500 (1981).